

**Correlation of Power Spectral Density with  
surface Quality of Fused Silica during  
Lapping and Polishing Process**



**By**

**Muhammad Mubisher Qasim**

**School of Chemical and Materials Engineering  
National University of Sciences and Technology**

**2022**

# **Correlation of Power Spectral Density with surface Quality of Fused Silica during Lapping and Polishing Process**



Name: Muhammad Mubisher Qasim

Registration No: 0000 273362

**This work is submitted as an MS thesis in partial fulfill the requirement**

**for the degree of**

**MS in Process Systems Engineering**

**Supervisor: Dr.Umair Sikander**

**School of Chemical and Materials Engineering (SCME)**

**National University of Sciences and Technology (NUST)**

**H-12 Islamabad, Pakistan**

**(2018-2022)**

# Declaration

I, **Muhammad Mubisher Qasim** declare that this thesis and the work presented in it are my own and has been generated by me as the result of my own original research. **Correlation of Power Spectral Density with surface Quality of Fused Silica during Lapping and Polishing Process.**

I confirm that:

1. This work was done wholly or mainly while in candidature for a research degree at this University;
2. Where any part of this thesis has previously been submitted for a degree or any other qualification at this University or any other institution, this has been clearly stated;
3. Where I have consulted the published work of others, this is always clearly attributed;
4. Where I have quoted from the work of others, the source is always given. With the exception of such quotations, this thesis is entirely my own work;
5. I have acknowledged all main sources of help;
6. Where the thesis is based on work done by myself jointly with others, I have made clear exactly what was done by others and what I have contributed myself;

Muhammad Mubisher Qasim

0000273362

## **DEDICATION**

TO MY HONORED PARENTS,  
RESPECTED TEACHERS, AND  
ALL THOSE WHO DEDICATED  
THEIR YESTERDAY TO  
MY BLESSED TODAY

# ACKNOWLEDGEMENT

Alhamdulillah, all praises to the **ALMIGHTY ALLAH** for his infinite blessings and strength in accomplishing this effort. All honour and respect are for his **HOLY PROPHET (PBUH)**, whose teachings are a great source of wisdom and guidance for the entire human race.

My special thanks goes out to **A.P. Dr. Umair Sikandar**, my supervisor, whose remarkable skills and scientific reasoning will always be unrivalled. His attempts to motivate me were not only for this thesis, but also for the rest of my life. For the completion of this task, I am grateful to his continual devotion and direction.

I'd like to thanks Dr. Ahsan, Dr. Iftikhar Salarzai, Dr. Salman Raza Naqvi and other faculty members for their informative conversations, encouragement, motivating guidance, and insightful recommendations that helped me finish this report.

My parents, siblings, and all of my friends, whose love and prayers have always been my greatest strength and inspiration, deserve my heartfelt gratitude and thanks.

# Table of contents

Abstract	vii
<b>1. Introduction</b>	<b>1</b>
1.1 Motivation	1
1.2 Fused Quartz and Soda-Lime-Silicate Glass	1
1.3 Fracture Studies Using Indentation	4
1.4 Types of Cracks Resulting from Indentations	5
1.5 Indentation Cracking Theories	5
1.6 Observations of Cracking in Brittle Materials	8
1.7 Outstanding Questions and Experimental Approach	15
<b>2. Literature Review</b>	<b>17</b>
2.1 Indentation	17
2.2 Contact between Elastic Solids	18
2.3 Elastic-plastic Contact	18
2.4 Indenters and Indentation Techniques	20
2.5 Load-displacement Curves	24
2.6 Factors Affecting Nano indentation Test Data	24
2.7 Chemo-mechanical polishing	25
2.8 Lapping	29
<b>3. Ansys Methodology</b>	<b>31</b>
3.1 ANSYS Methodology	31
3.2 Status of the cells	32
3.3 Engineering Data	34
3.4 Geometry	35
3.5 Meshing	37
3.6 Setup	38
3.7 Load Step and Sub Steps	40
<b>4. Results and Discussions</b>	<b>41</b>
4.1 Crack Formation and Evolution	41
4.2 Basic Governing Equations	42
4.3 Total deformation of different sizes	42
4.4 Equivalent Stress at different sizes	44
4.5 Total Deformation at different forces	45
4.6 Equivalent Stress at different forces	46
4.7 Comparison of FEA result with Experiments:	48
4.8 Pressure vs Total Deformation Curve:	49

<b>Conclusion</b>	<b>50</b>
<b>References</b>	<b>51</b>

## List of Figures

Figure 1-1 Different crack system due to projectiles	5
Figure 2-1 Vickers indentation test impression	21
Figure 2-2 Schematic showing rockwell hardness test	22
Figure 2-3 Schematic showing birnell hardness test	23
Figure 2-4 Load Depth	24
Figure 2-5 Schematic Diagram of CMP	26
Figure 2-6 CMP module	27
Figure 3-1 Ansys Methodology	32
Figure 3-2 Static Structural System	34
Figure 3-3 Geometry of model	36
Figure 3-4 Meshing of model	38
Figure 4-1 Basic Governing Equations	42
Figure 4-2 Total Deformation at different sizes	43
Figure 4-3 Equivalent stress at different sizes	45
Figure 4-4 Total Deformation at different forces	46
Figure 4-5 Equivalent stress at different forces	47
Figure 4-6 Comparison between calculated and measured load-depth data for three materials.	48

## **List of Tables**

Table 1-1 Cracking threshold load equations based on two different cracking theories	8
Table 2-1 Equation of normal pressure distribution	18
Table 3-1 Engineering data	35
Table 3-2 Boundary conditions model 1-4	36
Table 3-3 Boundary Conditions for Model 5-8	37
Table 3-4 Mesh Quality	38

## Abstract

Glassy materials has its application in various systems including electronics and semiconductors and optics. Particularly, in optics lens magnifications are produced by Lapping and Polishing process. These methods are used surface modification of fused silica by various indenters. In our work, alumina spheres are used as indenters. Load and stress graphs were plotted based on simulation results and were compared with literature. Studies for Total deformation and Equivalent stress at various indenters' size and loading pressures are carried out. It was observed that indenter sizes plays a vital role in cracks growth during lapping process. Minimizing subsurface damage (SSD) is in high demand for optics during grinding, lapping, and polishing. This study inspects and measures the SSD of fused silica developed in lapping. A series of simulations is conducted to reveal the influence of lapping parameters on SSD depth, including alumina size, lapping pressure. Results indicate that SSD depth are mostly sensitive to alumina size and lapping pressure. Indentation test is simulated using Finite Element Method based on contact mechanics approach. The relationship between load and indentation depth is obtained. The numerical results show good agreement with experimental data. It is shown that FEM is an effective tool for simulation of indentation tests of optics.

# Chapter No. 1

## 1. Introduction

### 1.1 Motivation

In a wide range of applications and industries, ceramic and glass materials are now being used in smaller volumes or in the form of thin films. There is a desire to have thinner glass surfaces to cover consumer electronics, durable ceramic coatings for biomedical applications, and lighter yet stronger windshields for military vehicles. In most applications in which brittle materials are being used, they undergo constant wear and erosion every day during the life of the device or coating. In some cases, the processing of ceramic and glass materials for such applications may introduce the same kind of impact to the surfaces, thus introducing flaws before the material is actually used. Because of the growing use of brittle materials for protective applications and every day devices, there is a need to fully understand how brittle materials fracture during small-scale contact and impact.

### 1.2 Fused Quartz and Soda-Lime-Silicate Glass

Before the 2000s, most indentation fracture studies were performed at high loads (1 N and above) using Vickers and spherical indenters [1, 2]. Glass has been an ideal material to study because of its transparent nature. Hagan and Swain successfully indented along a pre-crack and broke the pieces along this pre-crack to image the resulting fracture surfaces below the indentation impression [1]. Cook and Pharr built a indentation system over an inverted microscope to capture Fused quartz and soda-lime-silicate glasses are two common brittle materials that are being used

for some of the applications mentioned in the "Motivation" sub-section. Both glasses are different in composition and structure. Fused quartz is a network of SiO<sub>2</sub> with trace elements. Soda-lime- silicate glass is also a network of SiO<sub>2</sub>, except there is a higher abundance of additives when compared to fused silica or fused quartz [4]. In regards to their structures, fused silica has a less open SiO<sub>2</sub> network than soda-lime-silicate [4]. and document when cracking occurred entire loading and unloading cycle of the indentation process [2]. Two amorphous glasses that have been used in previous studies are fused silica (or also termed fused quartz) and soda-lime-silicate glass. Fused silica and fused quartz have been used interchangeably, however, the way they are processed may influence their final composition. For example, GE 124 fused quartz is still made up of SiO<sub>2</sub> like fused silica, but it has a lower OH content compared to fused silica [3]. Fused quartz and soda-lime-silicate glasses are two common brittle materials that are being used for some of the applications mentioned in the "Motivation" sub-section. Both glasses are different in composition and structure. Fused quartz is a network of SiO<sub>2</sub> with trace elements. Soda-lime- silicate glass is also a network of SiO<sub>2</sub>, except there is a higher abundance of additives when compared to fused silica or fused quartz [4]. In regards to their structures, fused silica has a less open SiO<sub>2</sub> network than soda-lime-silicate [4]. What researchers have found in the past is that both of these glasses crack differently during an indentation experiment. Fused quartz is termed an anomalous glass because it densifies during indentation and this densified region results in high tensile stresses that initiate cracks [5]. This densified region is the result of the material becoming compacted. Bridgman performed uniaxial compression tests on silicate glasses and observed that there is a pressure in which the glasses become compacted. Cohesive zone finite element analysis performed by Bruns et al. demonstrates that this densification does play a role in the resulting crack lengths after indentation experiments [7]. while soda-lime-

silicate is a normal glass where shear dominates the crack formation below the indentation impression [5]. Arora et al. found the deformation zones below the indentation impressions of fused silica and soda-lime-silicate to be different: soda-lime-silicate has shear lines in the area of the deformation zone, but fused silica does not [5]. Though both fused quartz and soda-lime-silicate glasses have been used in past indentation fracture experiments, fused quartz was chosen to be characterized in this study as opposed to soda-lime-silicate glass. As previously mentioned, there is a need to understand how brittle materials crack on the small-scales. To achieve the goal of providing a foundation of understanding, only one glass material the indentation impression [5]. Arora et al. found the deformation zones below the indentation impressions of fused silica and soda-lime-silicate to be different: soda-lime-silicate has shear lines in the area of the deformation zone, but fused silica does not [5]. Though both fused quartz and soda-lime-silicate glasses have been used in past indentation fracture experiments, fused quartz was chosen to be characterized in this study as opposed to soda-lime-silicate glass. As previously mentioned, there is a need to understand how brittle materials crack on the small-scales. To achieve the goal of providing a foundation of understanding, only one glass material needs to be selected. What researchers have found in the past is that both of these glasses crack differently during an indentation experiment. Fused quartz is termed an anomalous glass because it densifies during indentation and this densified region results in high tensile stresses that initiate cracks [5]. This densified region is the result of the material becoming compacted. Bridgman performed uniaxial compression tests observed that there is a pressure in which the glasses become compacted

### **1.3 Fracture Studies Using Indentation**

Extensive studies on the fracture of brittle materials have been performed, but it was not until the past thirty years that indentation has been used as a tool to investigate the fracture of materials. Indentation is a well developed technique in which fractured occurred in materials and resulting damage is analyzed using a microscope. Three sided pyramidal and conical indenters are typically used in indentation experiments. Vickers indenters are not usually used in indentation experiments because a chiseled edge would remain after trying to fabricate a four sided pyramidal indenter for the smaller scales. Two three sided pyramidal indenters that are typically used and available for users are the cube corner and Berkovich indenters. The Berkovich indenter is the three sided pyramidal indenter that is equivalent to the Vickers four sided pyramidal indenter. ]. The load at which a median crack nucleates depends on the size and location of the flaw below the surface [8]. Hagan, on the other hand, theorized that dislocation slip lines intersect one another below indentation impressions and it is at this intersection where a crack initiates [9, 10]. Dal Maschio et al. supported the theory that radial cracks initiate from the shear faults in the indentation impressions [11]. Swain studied and compared the indentation responses of fused silica and soda-lime glass. Not only did Swain present the different deformation zones below the indentations for the two glasses, Swain also concluded that the shear mechanism in the glasses was impeded by the amorphous, atomic structure [12]. The Berkovich indenter is the three sided pyramidal indenter that is equivalent to the Vickers four sided pyramidal indenter. ]. The load at which a median crack nucleates depends on the size and location of the flaw below the surface [8].

## 1.4 Types of Cracks Resulting from Indentations

The surface cracks that are observed in indentation experiments are termed radial cracks. These cracks typically propagate off of the corners of the indentations. Cracks that form below the impressions may be lateral, median, half-penny or cone cracks under the indentation impressions cracks appear on the surface.

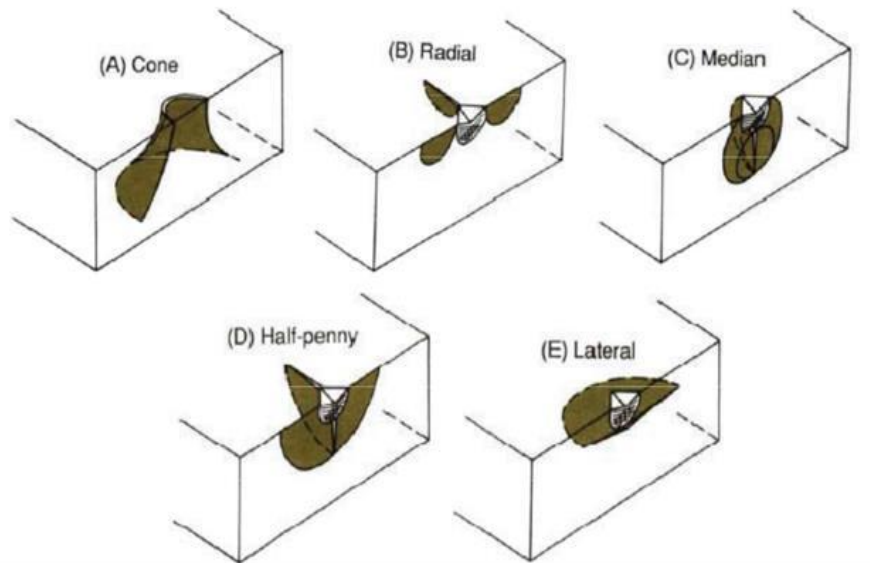


Figure 1-1 Different crack system due to projectiles

## 1.5 Indentation Cracking Theories

Observations of how surface and subsurface cracks nucleate in brittle materials have been previously presented by other researchers. Crack nucleation theories have been developed based on the observations of cracking in ceramics and glasses during and after Vickers indentation experiments. Lawn and Evans presented how a flaw below the indentation needs to be a certain size in order to initiate a median crack [8]. The load at which a median crack nucleates depends on the size and location of the flaw below the surface [8]. Hagan, on the other hand, theorized that

dislocation slip lines intersect one another below indentation impressions and it is at this intersection where a crack initiates [9, 10]. Dal Maschio et al. supported the theory that radial cracks initiate from the shear faults in the indentation impressions [11]. Swain studied and compared the indentation responses of fused silica and soda-lime glass. Not only did Swain present the different deformation zones below the indentations for the two glasses, Swain also concluded that the shear mechanism in the glasses was impeded by the amorphous, atomic structure [12]. With that conclusion drawn, Swain does not support the use of using the Lawn and Evans model to describe cracking in fused silica and soda-lime glasses [12]. Chiang et al. found in indentation studies performed at various loads that the load at which cracks did form is higher than the estimated cracking threshold load [13]. This supported Chiang et al.'s conclusion that the number of flaws surrounding the indentation impressions will influence the load at which cracking is observed on the surface of materials [13]. Up to this point, the crack nucleation theories have been based upon median and radial cracks. Tandon et al. performed a crack nucleation study on cone cracks in various transparent glasses using sharp, Vickers indenters to describe cracking in fused silica and soda-lime glasses [12]. Chiang et al. found in indentation studies performed at various loads that the load at which cracks did form is higher than the estimated cracking threshold load [13]. This supported Chiang et al.'s conclusion that the number of flaws surrounding the indentation impressions will influence the load at which cracking is observed on the surface of materials [13].

Zhuang et al.'s work demonstrates that different crack systems may be dependent on each other throughout the indentation cycle.

Up to this point, the crack nucleation theories have been based upon median and radial cracks.

Tandon et al. performed a crack nucleation study on cone cracks in various transparent glasses using sharp, Vickers indenters. Cone cracks were observed to form inside the deformation zone directly below the impression [15]. This means shear stresses are not contributing to the initiation and propagation of cone cracks [15].

In most recent years, finite elements and molecular dynamics have been used to understand crack nucleation. Luo et al. developed a molecular dynamic simulation that performed wedge indentations on oxide glass materials. One of the conclusions that was drawn from the simulation was that plasticity plays a role in fracture of glasses [16]. A second conclusion was cracks nucleate at the tip of the wedge indenter [16]. This second conclusion contradicts what others have observed experimentally. In the experimental studies that will be discussed in more detail later, the cracks were observed to nucleate near or at a point along the deformation zone below the indentation impression [17-19]. A third conclusion drawn was that cracks formed only under the sharper wedge indentations [16].

Along with the physical crack nucleation theories, researchers had attempted to develop equations and relationships to calculate the cracking load. The first model to calculate the cracking threshold load was developed by Lawn and Evans. The equation was developed with the assumptions that the tensile stresses below an indentation play a role in the nucleation of median cracks and a critical flaw size is needed to be met in order for the crack to form [8]. Hagan modified the model developed by Lawn and Evans to incorporate the shear stresses from dislocation lines. Both models Whittle and Hand analyzed the subsurface cracking patterns of Vickers indentations on soda-lime- silicate glasses. They made indentations on the surface and broke the glass using a four point bending method to cross section through the indentation for viewing [27]. They found

that the median/radial cracks were semi-elliptical in shape and influenced the lateral crack pattern [13]. Lateral cracks were closer to the surface of the material below the radial cracks; and as the lateral cracks propagated away from the radials, they went deeper into the material [23].result in different threshold loads,  $P_{th}$ , as shown in Table 1.1. The hardness,  $H_v$ , in Table 1.1 is the Vickers hardness.

Table 1-1 Cracking threshold load equations based on two different cracking theories

Source of cracking Threshold Load Equation	Cracking Threshold Load Equation
Lawn and Evens[8]	$P_{th} = 2.2 * 10^4 (K_{IG}/H_v)^3 K_{IG}$
Hagan[9]	$P_{th} = 885 (K_{IG}/H_v)^3 K_{IG}$

## 1.6 Observations of Cracking in Brittle Materials

The types of crack systems, cracking theories, and cracking threshold load estimations have been discussed previously. This sub-section will focus on providing a more in depth discussion on the most recent conclusions drawn about cracking below indentations in brittle materials. The sub- sections are organized in a way that points out the different tools used to capture the cracking of brittle materials. Whittle and Hand analyzed the subsurface cracking patterns of Vickers indentations on soda-lime- silicate glasses. They made indentations on the surface and broke the glass using a four point bending method to cross section through

the indentation for viewing [27]. They found that the median/radial cracks were semi-elliptical in shape and influenced the lateral crack pattern [13]. Lateral cracks were closer to the surface of the material below the radial cracks; and as the lateral cracks propagated away from the radials, they went deeper into the material [23]

### **1.6.1. Optical Microscopy:**

Viewing indentation impressions during and after indentation tests have primarily been performed using optical microscopes. Vickers and spherical indentations are typically large and are able to be imaged using optical microscopes because of their sizes. The following studies discussed are those that have utilized optical microscopes to characterize the cracking behavior of brittle materials. There are many researchers and other works that could be presented, but these studies are provided because the observations made in this study will be compared to the ones discussed here.

Whittle and Hand analyzed the subsurface cracking patterns of Vickers indentations on soda-lime-silicate glasses. They made indentations on the surface and broke the glass using a four point bending method to cross section through the indentation for viewing [27]. They found that the median/radial cracks were semi-elliptical in shape and influenced the lateral crack pattern [13]. Lateral cracks were closer to the surface of the material below the radial cracks; and as the lateral cracks propagated away from the radials, they went deeper into the material [23]. This shows that the lateral crack pattern below the indentation impressions depends on the median/radial cracks. Also, Whittle and Hand pointed out that lateral cracks do not lead to chipping in indentations because they propagate deeper into the material and do not appear to come back up to the surface away from the indentation impression[20].One conclusion drawn from his studies was mentioned

before and supported by other works: the sharper indenters induce more fracture in glass at lower loads [23]. From his studies, Gross pointed out that in some cases indentations performed under the same conditions cracked differently. As an example, Gross presented two indentations made on alumino-borosilicate glass with the same indenter and load. One of the indentations had no cracks and the other had cracks [23]. Gross' explanation is that the surface condition of the material and the number of flaws around the indentation site will play a role in how the indentations crack [23]. This observation was also made by Chiang et al. One conclusion drawn from his studies was mentioned before and supported by other works: the sharper indenters induce more fracture in glass at lower loads [23]. From his studies, Gross pointed out that in some cases indentations performed under the same conditions cracked differently. As an example, Gross presented two indentations made on alumino-borosilicate glass with the same indenter and load. One of the indentations had no cracks and the other had cracks [23]. Gross' explanation is that the surface condition of the material and the number of flaws around the indentation site will play a role in how the indentations crack [23]. This observation was also made by Chiang et al. which was introduced earlier in this chapter. Whittle and Hand analyzed the subsurface cracking patterns of Vickers indentations on soda-lime- silicate glasses. They made indentations on the surface and broke the glass using a four point bending method to cross section through the indentation for viewing [27]. They found that the median/radial cracks were semi-elliptical in shape and influenced the lateral crack pattern [13]. Lateral cracks were closer to the surface of the material below the radial cracks; and as the lateral cracks propagated away from the radials, they went deeper into the material [23]. This shows that the lateral crack pattern below the indentation impressions depends on the median/radial cracks.

### **1.6.1 Electron Microscopy and Focused Ion Beam Cross Sectioning**

The newest tool that is being used to cross section small indentations is the focused ion beam. Ions from the focused ion beam source (gallium ion source is one example) bombard the surface of a material and the material is removed from the surface exposing the subsurface. Dual beams with scanning electron and focused ion beam capabilities are best to use for imaging and milling.

Though edge cracks have been observed by some using optical microscopes, the edge cracking features are better to image using scanning electron microscopy due to the better resolution on the smaller scales. Xie et al. observed the Vickers indentation impressions on  $\beta$ -sialon inside a scanning electron microscope with a focused ion beam. In their studies, the edge cracks formed at lower loads before radial cracks formed at higher loads. The radial cracks were shallow, Palmqvist cracks as opposed to the half-penny cracks resulting from median cracks. There are some issues that may arise from milling indentations with a focused ion beam mill. Because the focused ion beam source is literally a foreign ion hitting the surface of the material being analyzed, caution needs to be taken and ensure there are no effects on the cracking due to the foreign ions. In some instances, the focused ion beam milling may introduce a feature in the cross section of interest called "curtaining". A "curtain" may form in the resulting cross section below a feature that is not smooth along the main surface being milled [35]. In other words, an obstruction (crack or hole) on the surface being milled would cause the ions to continue removing material below the obstruction. Focused ion beam milling allows a user to mill cross sections that are nanometers apart and observe how a crack appears below the entire indentation impression. In studies performed by Cuadrado et al., 3D constructions of the subsurface cracking below indentations

Focused ion beam milling allows a user to mill cross sections that are nanometers apart and observe how a crack appears below the entire indentation impression. In studies performed by Cuadrado et al., 3D constructions of the subsurface cracking below indentations were obtained using focused ion beam tomography [17]. This means the images from various cross sections throughout the indentation are stacked together in a software to provide a 3D view of the crack pattern.

There are some issues that may arise from milling indentations with a focused ion beam mill. Because the focused ion beam source is literally a foreign ion hitting the surface of the material being analyzed, caution needs to be taken and ensure there are no effects on the cracking due to the foreign ions. In some instances, the focused ion beam milling may introduce a feature in the cross section of interest called "curtaining". A "curtain" may form in the resulting cross section below a feature that is not smooth along the main surface being milled [35]. In other words, an obstruction (crack or hole) on the surface being milled would cause the ions to continue removing material below the obstruction. These "curtain" features may look like an extension of a crack or hole [35]. It is important to analyze the cross sections of indentations and determine whether or not the feature is a crack or a result of "curtaining". It is also important to be sure the cracks from indentations are not affected by the removal of material surrounding the indentations. Residual stresses may be introduced and cause cracks to propagate. There are some issues that may arise from milling indentations with a focused ion beam mill. Because the focused ion beam source is literally a foreign ion hitting the surface of the material being analyzed, caution needs to be taken and ensure there are no effects on the cracking due to the foreign ions. In some instances, the focused ion beam milling may introduce a feature in the cross section of interest called "curtaining". A "curtain" may form in the resulting cross section.

### **1.6.2 Finite Element Analysis**

Experimental observations of cracking in brittle materials has primarily been the focus in many experiments. However, finite element analysis can be used in conjunction with experimental findings or can be used on its own to characterize crack initiation and propagation. As it was introduced earlier, researchers have utilized finite element simulations to formulate fracture toughness relationships. Hyun et al. utilized cohesive zone finite elements to map out the crack shape below three sided pyramidal indentations. They found that there is not a crack that forms below the face of the three sided pyramidal indentations, but along the sharp, edge plane of the impression. An issue with using cohesive zone finite elements is that the user needs to specify the location of the indentation impression where cracks will propagate. Bruns et al. performed finite element simulations to analyze the effect of densification and indenter geometry on resulting cracking behaviors [7]. One of the conclusions drawn from Bruns et al.'s work was that densification plays a stronger role in the increase of crack lengths when the indenter becomes sharper [7]. Based on the findings, Bruns et al. discussed how the LEM fracture toughness equation does not account for densification and will not be an accurate model to estimate fracture toughness of materials that densify [7].

### **1.6.3 Molecular Dynamics**

Besides finite element analysis, molecular dynamics can be used to simulate an indentation experiment and obtain information on the crack initiation and propagation. Yang et al. used Yang et al. explained the need to study the cracking process of metallic glass materials using

molecular dynamics. The authors mentioned the difficulty in capturing the cracks below the surface of the indentations in metallic glasses using optical methods that are used for transparent glasses [37]. With that said, molecular dynamics has been proposed as a useful tool to characterize the initiation and propagation of cracks in materials that cannot be studied using traditional microscopy methods. However, caution needs to be taken whenever utilizing a simulation or theory to explain a phenomenon without any experimental observations. molecular dynamic simulations to better understand the crack initiation and propagation in metallic glass materials [37]. Yang et al. explained the need to study the cracking process of metallic glass materials using molecular dynamics. The authors mentioned the difficulty in capturing the cracks below the surface of the indentations in metallic glasses using optical methods that are used for transparent glasses [37]. With that said, molecular dynamics has been proposed as a useful tool to characterize the initiation and propagation of cracks in materials that cannot be studied using traditional microscopy methods. However, caution needs to be taken whenever utilizing a simulation or theory to explain a phenomenon without any experimental observation. molecular dynamic simulations to better understand the crack initiation and propagation in metallic glass materials [37]. Yang et al. explained the need to study the cracking process of metallic glass materials using molecular dynamics. The authors mentioned the difficulty in capturing the cracks below the surface of the indentations in metallic glasses using optical methods that are used for transparent glasses [37]. With that said, molecular dynamics has been proposed as a useful tool to characterize the initiation and propagation of cracks in materials that cannot be studied using traditional microscopy methods. However, caution needs to be taken whenever utilizing a simulation or theory to explain a phenomenon without any experimental observations

## 1.7 Outstanding Questions and Experimental Approach

Though indentation has been used to characterize the cracking behavior of glasses, there is still a need to explore when and how brittle materials crack on the small-scale. It has been demonstrated by Harding and Morris and Cook that the indenter angle geometry can change the cracking threshold load.

Fracture toughness of brittle materials have been calculated using indentation. There are, however, two equations that are being used: one developed by Lawn, Evans and Marshall (LEM) and the other developed by Laugier. The LEM model is to be used for indentations with well developed half-penny cracks and the Laugier model is to be used for indentations with Palmqvist cracks. In addition to these models, Jang and Pharr have solved for the indenter angle dependence of the constant in the LEM model. A question that arises from these previous works is which model Indentation impressions are very small and are typically in the size range of 0.5  $\mu\text{m}$  to 10  $\mu\text{m}$  (including the length of the cracks). These indentations are too small to be pre-cracked and cross sectioned using the bending method. Experimental works (like those performed by Cuadrado et al.) and cracking studies using simulation (like those performed by Luo et al.) have resulted in different conclusions as to how cracks form during indentation. There is a need to better understand how cracks form and evolve below indentation impressions at smaller loads (below 500 mN).should be used to estimate the fracture toughness in indentation experiments? Can the fracture toughness be calculated using indenters of different angle?The fracture toughness equations that have been proposed will be compared and a conclusion will be drawn about which models work best for the fused quartz material. By using a new tool, the focused ion beam mill

In this work, crack initiation and evolution of fused quartz are studied using indentation, focused ion beam mill, and finite elements. Fused quartz is the chosen material because it is the common reference brittle material. By changing the indenter geometry, the cracking threshold load can be captured on the small-scales.

# Chapter # 2

## 2. Literature Review

### 2.1 Indentation

The mechanical properties of material is determining by indentation method.. Indentation testing is the process of contacting a material with unknown mechanical properties (such as elastic modulus and hardness) with a material with known mechanical qualities. The approach is based on the Mohs mineral hardness scale, which was first published in 1812 [1, 2]. In a typical indentation test, the penetration length is measured in microns or millimetres. Nanoindentation, a type of indentation test in which the penetration length is measured in nanometers, has recently emerged as a standard tool for assessing the mechanical properties of small volumes of material [3-5]. Hardness, elastic modulus, strain-hardening exponent, fracture toughness (for brittle materials), and viscoelastic characteristics can all be calculated using the nanoindentation technique [6]. In comparison to elastic-plastic stress fields, indenter-generated elastic stress fields are comparatively simple. Due of their complexity, the above-mentioned theoretical treatments are In elastic-plastic (e.g. metal) and brittle (e.g. ceramics, glass) materials, the permanent indentation formed can be measured to represent the indentation resistance (i.e. hardness of the material) Giannakopoulos and Larsson (1997), whereas in a soft material (e.g. rubber, foam), the permanent indentation formed can be measured to represent the indentation resistance.

## 2.2 Contact between Elastic Solids

Numerous assumptions are made in the analysis of the indentation process and the contact between elastic material.. The dimensions of each body are huge when compared to the radius of the contact circle. If this assumption is correct, each surface can be thought of as an elastic half space.. Frictionless contact exists between the two bodies. Between the indenter and the specimen, only normal pressure is communicated.

Table 2-1 Equation of normal pressure distribution

Indenter Type	Equation for Normal Pressure Distribution
Sphere	$P_m = -\frac{6Z}{2} (1 - r^2/a^2)^{1/2}$
Cone	$\frac{6Z}{P_m} = -\frac{\cosh^{-1}a}{r}$

## 2.3 Elastic-plastic Contact

In comparison to elastic-plastic stress fields, indenter-generated elastic stress fields are comparatively simple. Due of their complexity, the above-mentioned theoretical treatments areIn elastic-plastic (e.g. metal) and brittle (e.g. ceramics, glass) materials, the permanent indentation formed can be measured to represent the indentation resistance (i.e. hardness of the

material) Giannakopoulos and Larsson (1997), whereas in a soft material (e.g. rubber, foam), the permanent indentation formed can be measured to represent the indentation resistance (i.e. hardness of the material) Giannakopoulos the hardness of the material is measured limited in the case of elastic-plastic issues. Elastic-plastic indentations are commonly studied using numerical approaches such as the finite element method [11]. The mechanical properties of material is determining by indentation method.. Indentation testing is the process of contacting a material with unknown mechanical properties (such as elastic modulus and hardness) with a material with known mechanical qualities. The approach is based on the Mohs mineral hardness scale, which was first published in 1812 [1, 2]. In a typical indentation test, the penetration length is measured in microns or millimetres. Nanoindentation, a type of indentation test in which the penetration length is measured in nanometers, has recently emerged as a standard tool for assessing the mechanical properties of small volumes of material [3-5]. Hardness, elastic modulus, strain-hardening exponent, fracture toughness (for brittle materials), and viscoelastic characteristics can all be calculated using the nanoindentation technique [6].

In comparison to elastic-plastic stress fields, indenter-generated elastic stress fields are comparatively simple. Due of their complexity, the above-mentioned theoretical treatments areIn elastic-plastic (e.g. metal) and brittle (e.g. ceramics, glass) materials, the permanent indentation formed can be measured to represent the indentation resistance (i.e. hardness of the material) Giannakopoulos and Larsson (1997), whereas in a soft material (e.g. rubber, foam), the permanent indentation formed can be measured to represent the indentation resistance.

## 2.4 Indenters and Indentation Techniques

For a long time, indentation testing, also known as hardness testing, has been regarded a standard procedure for material characterization. The indenter of a hardness test equipment is often composed of diamond or a hard material such as tungsten carbide, which is pressed into the surface of the material during the loading stage and force displacement data is utilised to indicate the material's resistance. In elastic-plastic (e.g. metal) and brittle (e.g. ceramics, glass) materials, the permanent indentation formed can be measured to represent the indentation resistance (i.e. hardness of the material) Giannakopoulos and Larsson (1997), whereas in a soft material (e.g. rubber, foam), the permanent indentation formed can be measured to represent the indentation resistance (i.e. hardness of the material) Giannakopoulos the hardness of the material is measured by the indentation depth under load, Ren X. J. (2001). Many factors, including experimental settings, mechanical and physical properties of materials, and indenter geometry, can affect indentation hardness. When employing the indentation technique for material characterization, several considerations should be carefully examined. One of the most significant aspects of indentation testing is the indenter geometry. Pyramidal, conical, and spherical form indenters are some of the most frequent types of indenters used in the indentation process. The shape of the indenter affects the hardness of a material system. The five major standard test techniques for proving the connection between hardness and the size of the imprint are Vickers hardness, Berkovich hardness, Knoop hardness, Rockwell hardness, and Brinell hardness testing. The next sections go through different indentation methods in more detail.

### 2.4.1 Vickers hardness test

The Vickers indenter is a diamond pyramidal-shaped square with a 136-degree angle between the faces and a 1:1 diagonal ratio. In engineering and materials research one of the most widely used hardness measures is the Vickers hardness number.. The Vickers hardness, HV, is determined by multiplying the indenter load F by the diagonals, d, of the impression area left on the specimen's surface when the indenter is removed. The average value of d is measured using a microscope attached to the hardness equipment. As most cases, the resultant quantity is represented Where F is the load in kgf, d1 and d2 are the two diagonals' mathematical expressions, and HV is the Vickers hardness.in, $kgf/mm^2$ . Where F is the load in kgf, d1 and d2 are the two diagonals' mathematical expressions, and HV is the Vickers hardness.

$$H_V = \frac{2F \sin \frac{136}{2}}{d^2} = 1.854F/d^2$$

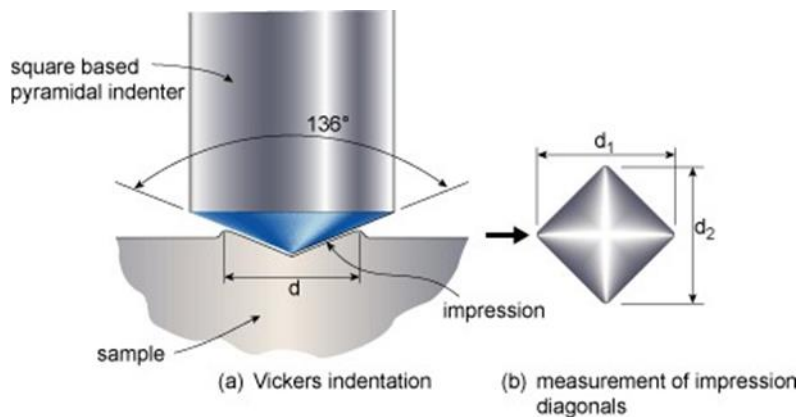


Figure 2-1 Vickers indentation test impression

## 2.4.2 Rockwell hardness

The Rockwell hardness test method uses a diamond cone or spherical indenter to determine the indentation hardness of test materials. The indenter is loaded onto the test material under a little load until a balance is reached, after which the indenter is moved under a big load and the difference in penetration depth of the indenter is compared to a datum point. The new major load is withdrawn once equilibrium has been restored, but the initial minor load is kept. Due to the elimination of the additional significant load, a partial recovery occurs, resulting in a reduction in penetration depth. calculate the Rockwell hardness number given by equation

$$HR = E - e$$

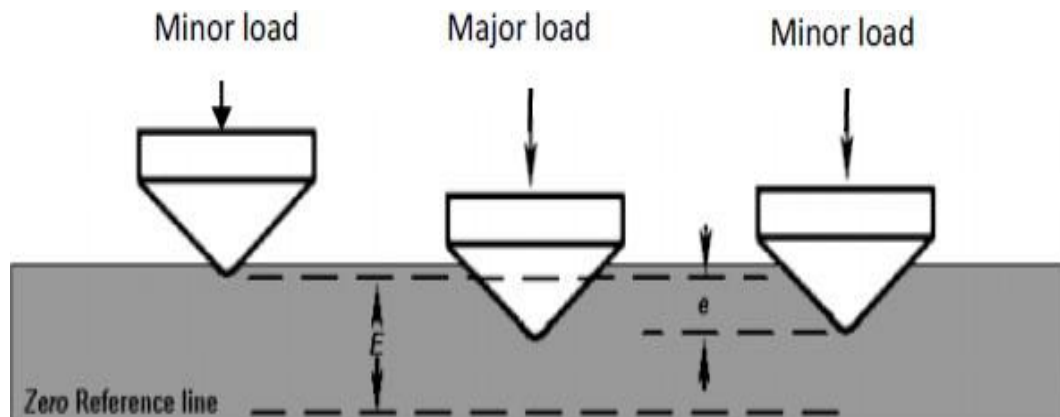


Figure 2-2 Schematic showing rockwell hardness test

## 2.4.3 Brinell hardness

The Brinell hardness test method determines the indentation hardness of a test material using a spherical indenter of carbide or hardened steel, typically 10mm in diameter, D, pressed with 30

KN force,  $F$ , for a period of 10 to 15 seconds in the case of steel, and 30 seconds or more in the case of other metals, for a period of 10 to 15 seconds in the case of steel, and 30 seconds or more in the case of other metals. When the indenter is withdrawn, a low-powered optical microscope is used to measure the diameter,  $d$ , of the impression area left on the specimen's surface. The Brinell hardness number is calculated by dividing the force applied by the projected spherical surface area of the indentation tip.

$$H_B = \frac{2F}{\pi D} (D - \sqrt{D^2 - d^2})$$

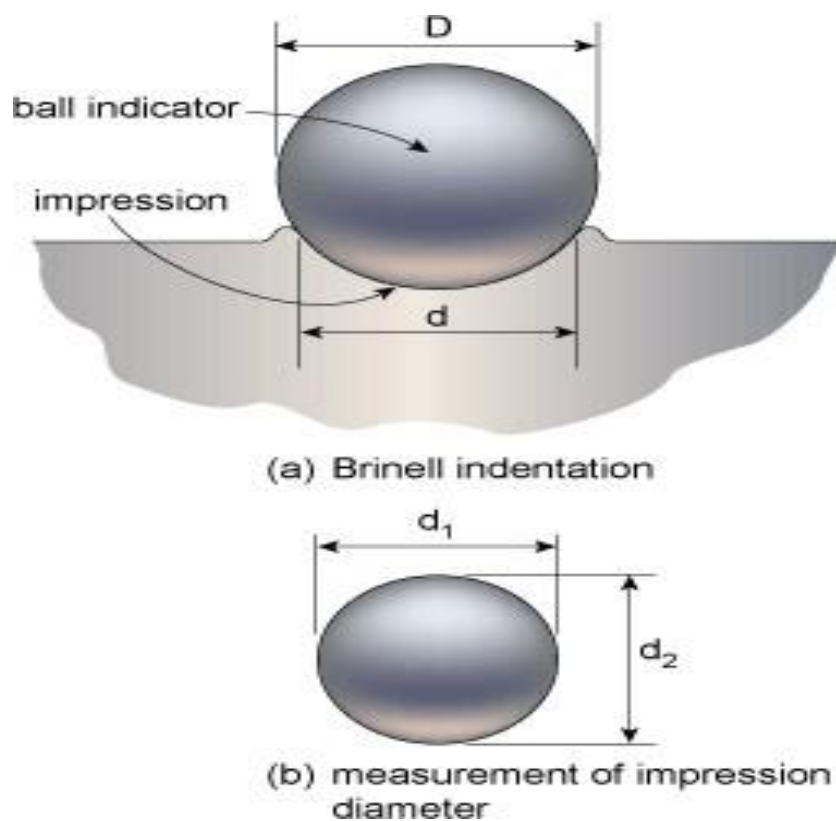


Figure 2-3 Schematic showing Brinell hardness test

## 2.5 Load-displacement Curves

The load and depth of penetration are recorded in a typical nanoindentation test. The load is applied in incremental increments from zero to a maximum value during the loading process. The load then drops from its greatest value to zero throughout the unloading procedure. If the specimen deforms due to plastic deformation, a residual distortion is left on the surface. Optical approaches cannot accurately assess the residual deformation for nanoindentation testing because the size of the residual deformation is so small.

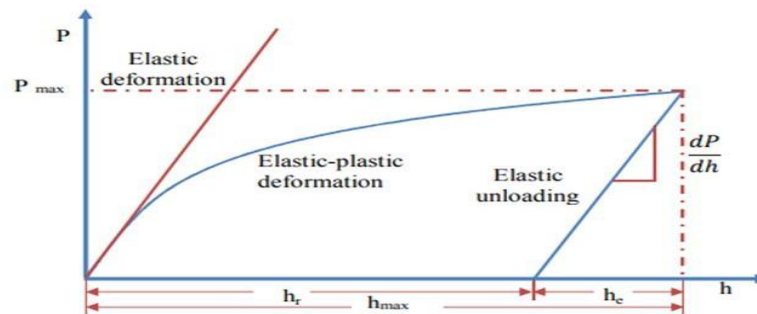


Figure 2-4 Load Depth

## 2.6 Factors Affecting Nano indentation Test Data

The Nano indentation testing process is prone to a variety of mistakes [14, 16-20]. The validity of the results will be influenced by offsets in depth measurements, environmental changes during the test, the non-ideal shape of the indenter, and some material-related difficulties, for example. The following are some of the most prevalent factors encountered in experimental and numerical. The initial contact force, which results in initial penetration, is set at around 1 N in the experiments. To avoid this inaccuracy, all displacement measurements must include a tiny initial

depth [1]. Indenter geometry: The geometry of the indenter may not be optimal in practise. . The standard shape of a diamond indenter can be affected by a variety of circumstances, including crystal anisotropy

Analysis. In a Nano indentation test, the indenter displacement should ideally be measured from the specimen's top surface. In practice, however, the indenter must first make contact with the specimen surface before displacement measurements can be taken. As a result, an initial contact depth appears, which is normally set as low as possible. The initial contact force, which results in initial penetration, is set at around 1 N in the experiments. To avoid this inaccuracy, all displacement measurements must include a tiny initial depth [1]. Indenter geometry: The geometry of the indenter may not be optimal in practice. . The standard shape of a diamond indenter can be affected by a variety of circumstances, including crystal anisotropy. As a result, a correction factor is required to address the issues produced by the indenter's non-ideal geometry in practical tests [1]. AFM or SEM measurements of the indenter geometry can be used to calculate the correction factor. The indenter's area function can also be calculated [21]. Pile-up and sink-in: When plastic deformation occurs, the specimen material may either sink in or pile-up around the indenter [3, 18].

## **2.7 Chemo-mechanical polishing**

Chemical-Mechanical-Polishing (CMP), a planarization process first developed and used for the manufacturing of multi-level metal interconnects for high-density Integrated Circuits (IC), has been adapted as an enabling technology in the fabrication of microelectromechanical systems (MEMS) or more generally, microsystems technology (MST). The CMP planarization technique

alleviates many manufacturing issues introduced by topography generated during the fabrication of multi-layer MST structures. Historically, this was specifically true with polysilicon surface micromachining, an additive manufacturing technology, which was comprised of as many as six added levels of polysilicon. Such a technology would not have been possible without the incorporation of CMP planarization between layers. For the designer, CMP not only eliminates design constraints introduced by non-planar topography generated at intermediate fabrication steps, but also improves the overall quality of surfaces and potentially provides an avenue for integrating disparate process technologies.

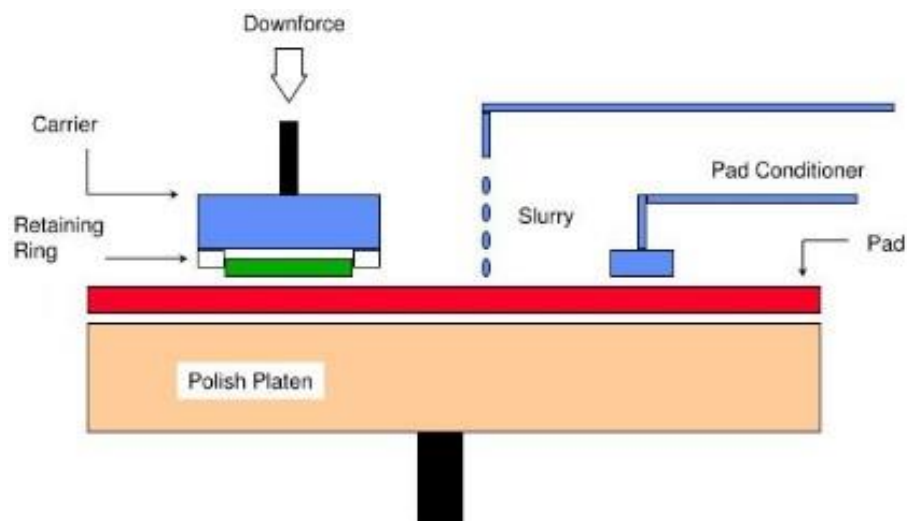


Figure 2-5 Schematic Diagram of CMP

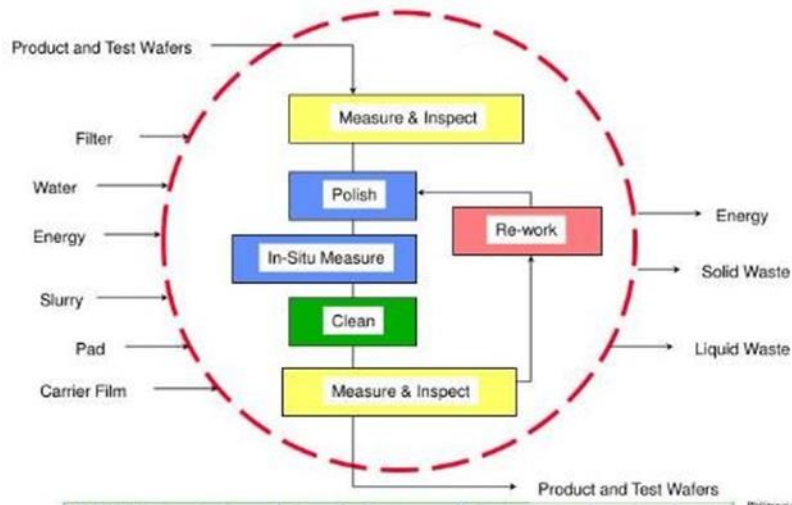


Figure 2-6 CMP module

### 2.7.1 CMP limitations

The principle limitation of CMP is total material removal, (i.e., height of topography removed). CMP provides a high quality finish with little substrate damage, but it is relatively slow at material removal and, therefore, becomes an expensive process as film thickness increases. Typical film removal can be in the sub-micron to several microns thickness. If significantly greater material must be removed, an initial removal using mechanical grinding or lapping followed by CMP to remove the damaged material and provide a high quality finish is an alternative process. For example, mechanical grinding can have removal rates of approximately 100 microns of Si in 6 minutes versus 0.65 micron SiO<sub>2</sub> in 2.5 minutes with CMP. Mechanical polishing alone is unacceptable in many cases and, most specifically, for semiconductor IC processing due to excessive mechanical damage to the wafer surface. Although one may think that this is not essential to micromechanical devices and structures, the damage can lead to mechanical stress gradients in layers that, upon release to form free-standing structures, generate undesired structural

deformation (i.e., curvature of plates and beams). Again, strain gradients in layers and the resulting deformation are process parameters of which a designer must inquire at the foundry of choice. .

If significantly greater material must be removed, an initial removal using mechanical grinding or lapping followed by CMP to remove the damaged material and provide a high quality finish is an alternative process. For example, mechanical grinding can have removal rates of approximately 100 microns of Si in 6 minutes versus 0.65 micron SiO<sub>2</sub> in 2.5 minutes with CMP. Mechanical polishing alone is unacceptable in many cases and, most specifically, for semiconductor IC processing due to excessive mechanical damage to the wafer surface. Although one may think that this is not essential to micromechanical devices and structures, the damage can lead to mechanical stress gradients in layers that, upon release to form free-standing structures, generate undesired structural deformation (i.e., curvature of plates and beams). The principle limitation of CMP is total material removal, (i.e., height of topography removed). CMP provides a high quality finish with little substrate damage, but it is relatively slow at material removal and, therefore, becomes an expensive process as film thickness increases. Typical film removal can be in the sub-micron to several microns thickness. If significantly greater material must be removed, an initial removal using mechanical grinding or lapping followed by CMP to remove the damaged material and provide a high quality finish is an alternative process. For example, mechanical grinding can have removal rates of approximately 100 microns of Si in 6 minutes versus 0.65 micron SiO<sub>2</sub> in 2.5 minutes with CMP. Mechanical polishing alone is unacceptable in many cases and, most specifically, for semiconductor IC processing due to excessive mechanical damage to the wafer surface.

## **2.8 Lapping**

Abrasive compounds like aluminum oxide, emery, and silicon carbide are used to grind the work piece and remove stock from the surface during lapping. Lapping is a technique for creating exceptionally flat, smooth, completed, and polished surfaces and edge faces. For precision thickness and surface finish items made of ceramics and metal alloys, lapping methods utilizing silicon carbide and aluminum oxide fine powders provide high volume procedures.

### **2.8.1 Fused Silica Polished method**

Cerium oxide is used as a polishing agent in the most common process for polishing fused silica. To avoid a thin coating of ceria-silica on the surface of fused silica, a new polishing procedure was developed, which combines alumina and silica as polishing chemicals.

### **2.8.2 Alumina polishing methods**

Alpine Research Optics (ARO) used a loose alumina abrasive lapping approach to remove material, with the goal of reducing subsurface damage during the lapping and polishing procedures. 9 Al<sub>2</sub>O<sub>3</sub> particles were used in the lapping process, followed by 5 Al<sub>2</sub>O<sub>3</sub> particles. Following final lapping, the work surfaces were examined with a 10x objective to ensure that all macro damage had been eliminated and that the surfaces were clean enough to commence the pre-polish process. The “Pre-Polish” process was completed by ARO utilizing Ultra Sol-M5-PS (an alumina polishing compound) and a 0.8-alumina slurry. To avoid “Oran,” the pH of the slurry was kept at 8. What effect can an acidic slurry have on fused silica? The fused silica windows

were polished further with smaller sized slurries once the "Pre-Polish" was accomplished, with the last process using a 100-nm slurry. The fused silica windows' surfaces were examined to check if they passed the 10-5 "Laser Quality" inspection. The surface quality of the fused silica window was determined to be marginally better than the 10/5 S/D following the last alumina polishing.

# Chapter # 3

## 3. Ansys Methodology

### 3.1 ANSYS Methodology

- When executing a finite element analysis, you must accomplish a number of activities, which can be thought of as the analysis' steps. These procedures must be completed regardless of whatever FEA tool is being used to accomplish the analysis. These tasks are stated below.
- ANSYS is a finite element analysis package used widely in industry to simulate the response of a physical system to structural loading, thermal and electromagnetic effects.
- ANSYS uses the finite-element method to solve the underlying governing equations and the associated problem-specific boundary conditions. The Ansys software simulates and analyzes movement, fatigue, fractures, fluid flow, temperature distribution, electromagnetefficiency and other effects over time.

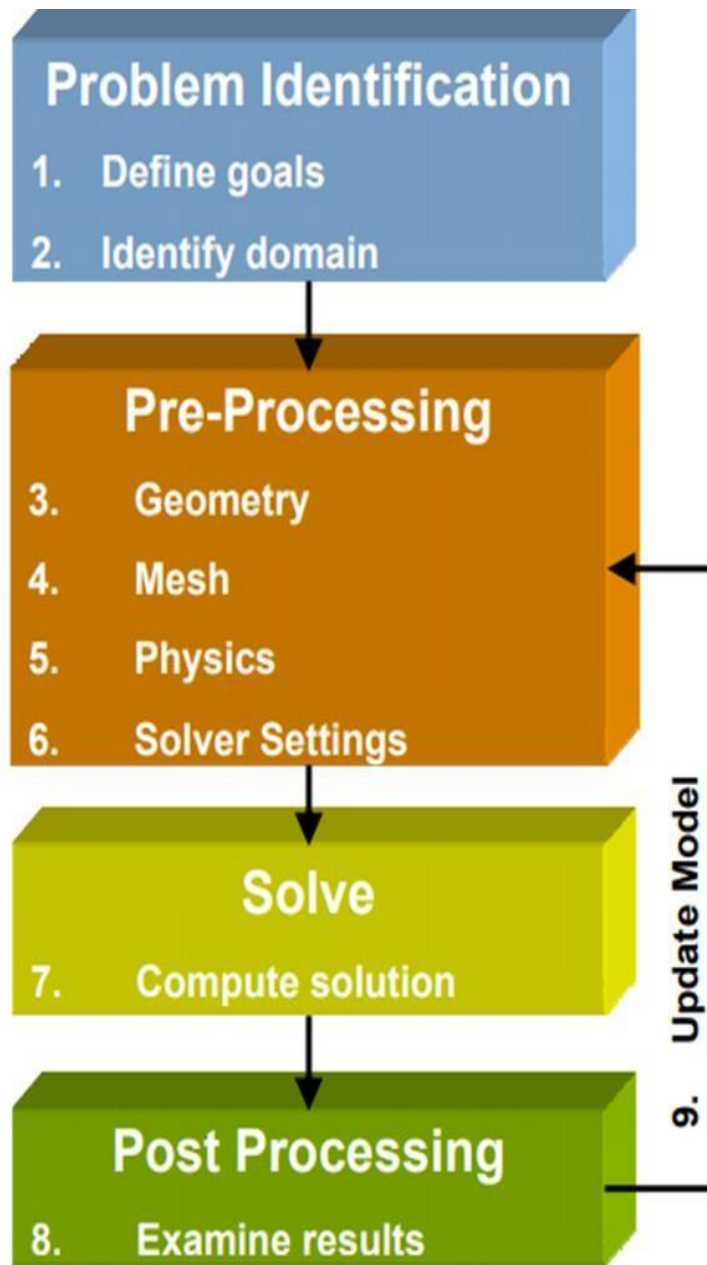


Figure 3-1 Ansys Methodology

### 3.2 Status of the cells

The icons appearing on the right side of each cell indicate the status of that cell as described in the following table.

<b>Icon</b>	<b>Meaning</b>
	It is necessary to pay attention. It could indicate that no upstream data, such as geometry, is currently available.
	Unfulfilled. The Attention Required icon will appear upstream of the current cell.  Before you can proceed, you must bring the upstream cell up to date.
	It's time to refresh. This indicator indicates that the data upstream has changed.  To decide what action to take, use the context menu.
	It's time to update. This indicator indicates that changes within this cell have occurred, necessitating the regeneration of the cell's output.
	This cell's data is fresh and can be passed on to downstream cells.

Start Workbench then start a new Static Structural analysis project by double-clicking on the icon in the Toolbox. Once the Static Structural System appears in the Project Schematic area, double-click on Geometry to start a new DesignModeler session.

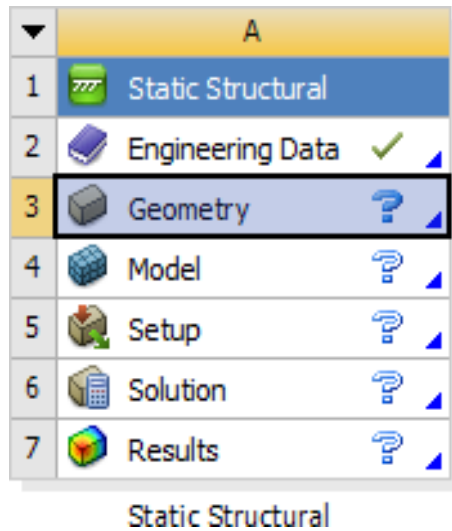


Figure 3-2 Static Structural System

### 3.3 Engineering Data

The material property definitions for the analysis are represented in this cell. Workbench makes the assumption that everything in our model is constructed of structural steel by default. As a result, if the part in our analysis is made of a different material, we must change Workbench's material assign to it.

Table 3-1 Engineering data

<b>PROPERTIES</b>	<b>FUSED SILICA</b>	<b>ALUMINA</b>
DENSITY(g/cm <sup>3</sup> )	2.20	3.69
SPECIFIC HEAT(j/kg)	0.770	870
YOUNG'S MODULUS(GPa)	73	275
BULK MODULUS(Pa)	3.5784e10	1.6369e11
SHEAR MODULUS(Pa)	3.1466e10	1.217e11
POISSON RATIO	0.16	0.22

### **3.4 Geometry**

This cell reflects the part or assembly to be analyzed solid model. Design Modeler may import geometry from another CAD programme or create it custom. Model, Setup, Solution, and Results. By default, the Mechanical Application handles all of these cells' data (formerly Simulation). As a result, double-clicking on any of these cells brings up the relevant object in the Mechanical Application interface's project tree. The 3D models were created and meshed by Ansys18.1. We supposed that all the mgeoodels use the same materials (Rectangle-shaped is Fused silica & Sphere-Shaped is Alumina). Nano indentation of fused silica and alumina materials with spherical indenters of various diameters is simulated using models 1,2,3, and 4. Models 5,6,7, and8 are used to simulate Nano indentation on fused silica and alumina materials, respectively, using

spherical indenters of various forces. The simulations are based on a few simple assumptions. To begin, the fused silica and alumina contact is considered to be properly connected.

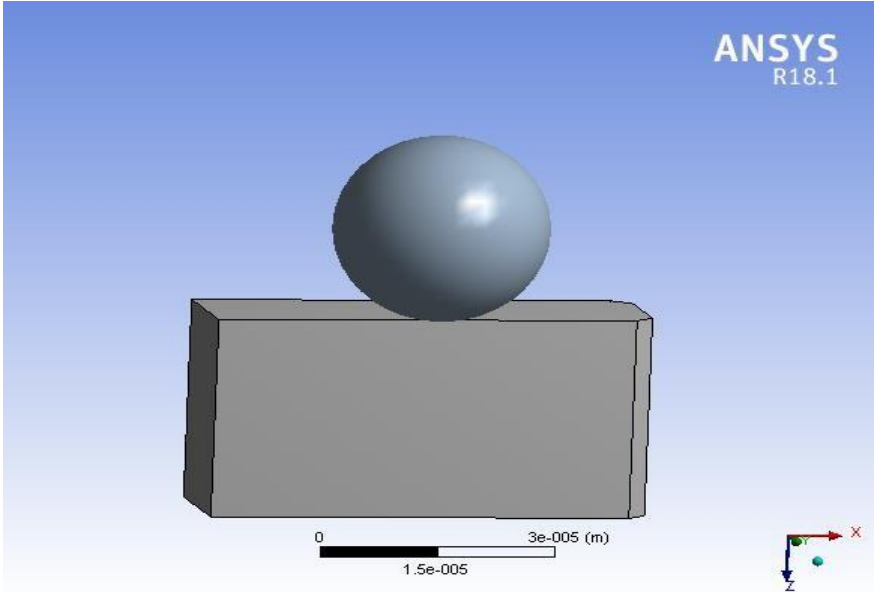


Figure 3-3 Geometry of model

Table 3-2 Boundary conditions model 1-4

	<b>FUSED SILICA</b>	<b>ALUMINA</b>	<b>PRESSURE</b>
<b>MODEL 1</b>	6529	18	1
<b>MODEL 2</b>	6529	14	1
<b>MODEL 3</b>	6529	10	1
<b>MODEL 4</b>	6529	5	1

In model 5,6,7,8 load applied on spherical indenter is vary but the size of the indenter is same

Table 3-3 Boundary Conditions for Model 5-8

	<b>FUSED SILICA</b>	<b>ALUMINA</b>	<b>PRESSURE</b>
<b>MODEL 5</b>	6529	10	2
<b>MODEL 6</b>	6529	10	4
<b>MODEL 7</b>	6529	10	6
<b>MODEL 8</b>	6529	10	8

### **3.5 Meshing**

When dealing with a minor displacement and a big force, mesh density and refinement are critical for improving model accuracy. As a result, the region of interest was employed comparably denser along the periphery of the indenting area because deformation during the indentation process is largely concentrated towards that region. However, because to limitations in the present version of the ANSYS programme, a large number of elements could not be used in the current 3-D model. Meshing of model 1,2,3 and 4 are shown in fig

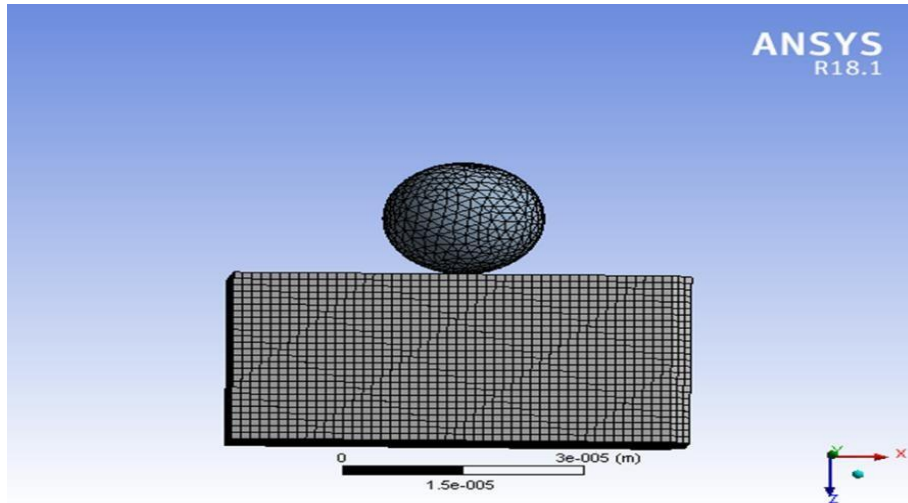


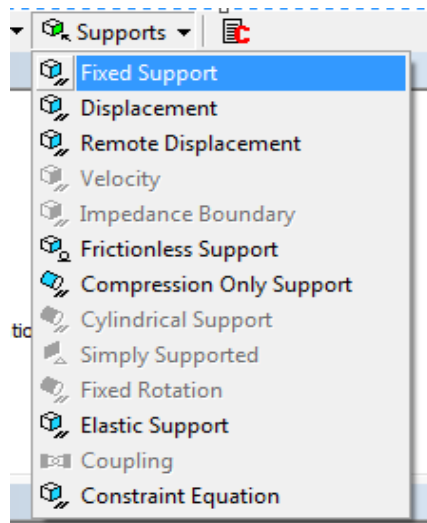
Figure 3-4 Meshing of model

Table 3-4 Mesh Quality

<b>Mesh Quality</b>	<b>Fused Silica</b>	<b>Alumina</b>
<b>Nodes</b>	86921	5071
<b>Elements</b>	19864	2990
<b>Average</b>	0.977	0.7877
<b>Standard Deviation</b>	3.514e-02	0.117

### 3.6 Setup

In “Setup”, the loads, the supports and the desired solution parameters should be defined. By marking the location on the geometry and adding a force or a support, the “Setup” stage can be considered to be done. Add the “Fixed Support” from the “Supports List”. Hence, on the “Outline” tree, the fixed support will be displayed under the “Static Structural” list.



Add the force from the “Loads” list. In the “Details of Force” window, change “Defined By” to “Components” and then set the “Y” direction force to be “ -1000N” as it is shown in the figure. The negative sign of the force is because the force is downwards. Always make sure you check the coordinate system defaults directions before setting the forces.

Details of "Force"	
<b>Scope</b>	
Scoping Method	Geometry Selection
Geometry	1 Edge
<b>Definition</b>	
Type	Force
Define By	Components
Coordinate System	Global Coordinate System
<input type="checkbox"/> X Component	0. N (ramped)
<input checked="" type="checkbox"/> Y Component	-1000
<input type="checkbox"/> Z Component	0. N (ramped)
Suppressed	No

After defining the investigation parameters, click solve to get the results. To show the results of the different parameters, use the list under “solutions” in the “Outline” window.

### **3.7 Load Step and Sub Steps**

Loading and unloading are the two load phases employed in the models. The loading behaviour of Nano indentation is reproduced by incrementally increasing the indenter displacement. The indenter is displaced in the z direction during the loading process, contacting the bulk material or thin film up to the maximum indentation depth. During the unloading process, the indenter gradually returns to its former location. In this load stage, the y direction displacement applied to the indenter is set to zero. The greatest number of sub steps that can be used to solve these nonlinear large strain issues cannot be too small.

# Chapter # 4

## 4. Results and Discussions

### 4.1 Crack Formation and Evolution

An important key observation made from the surface and subsurface cracking analysis of fused quartz during nanoindentation is that there is a distinct cracking threshold load for various cracks. Radial crack threshold load for fused quartz increased with indenter angle summarizes the radial cracking threshold loads for the different indenter loads used in this study and compares them to other studies:

To the best of the author's knowledge, there is not another study that has been performed looking at the cracking threshold load of fused quartz using the same indenters and load ranges. However, by looking at data found from Harding and Morris and Cook, it is clear that there are differences in the observations made by the different researchers. Comparison demonstrates is that there may be other factors influencing the cracking threshold load. Going back to the original cracking theories, Lawn and Evans described that crack initiation begins when a flaw reaches a critical size [8]. Hagan, on the other hand, described cracks to form by dislocation slip lines intersecting below the indentation impression [9]. As shown in the crack length and indentation load relationship there is not a lot of scatter in the crack length data. If flaws played a role in the cracking behavior of the indentations in fused quartz, then there would be a lot of scatter in the crack length measurements and it would be difficult to pin point the radial cracking threshold load. Therefore,

the crack nucleation theory developed by Hagan may be the best way to describe how cracks nucleate in fused quartz.

## 4.2 Basic Governing Equations

The governing equation clearly shows that initiation and growth of cracks is directly proportional to applied load on indenters. As we increase the load on indenter the cracks growth increased. From simulation result we observed that depth increase as load increase on indenters.

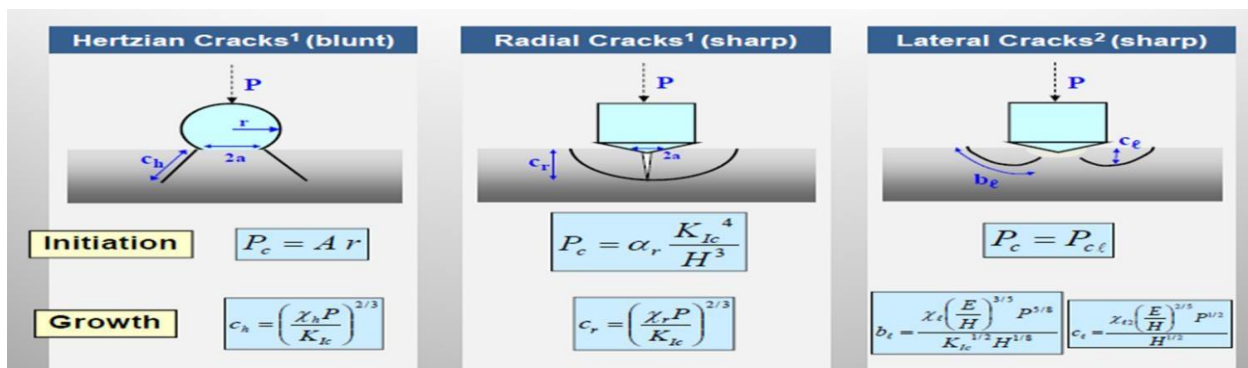


Figure 4-1 Basic Governing Equations

## 4.3 Total deformation of different sizes

Deformation results generally can be in ANSYS WorkBench as total deformation or directional deformation. In total deformation, it gives a square root of the summation of the square of x-direction, y-direction and z-direction. The maximum total deformation in fused silica by the impact of 18µm and 5µm alumina is 1.9546e-9m and 3.589e-10m respectively .I observed that total deformation is increases as the size of indenter increase its because of increasing the contact areaof indenter and surface of the body.

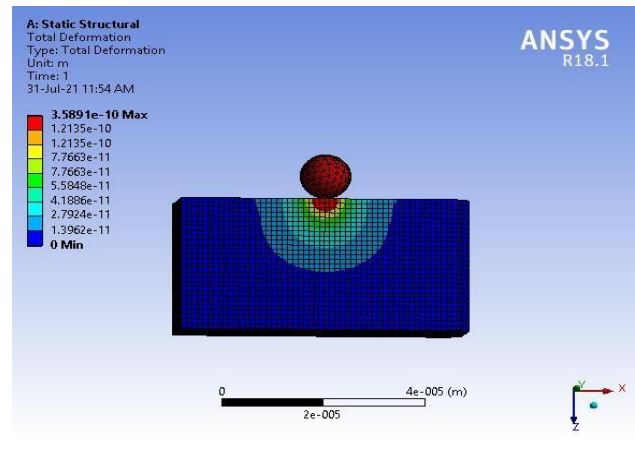
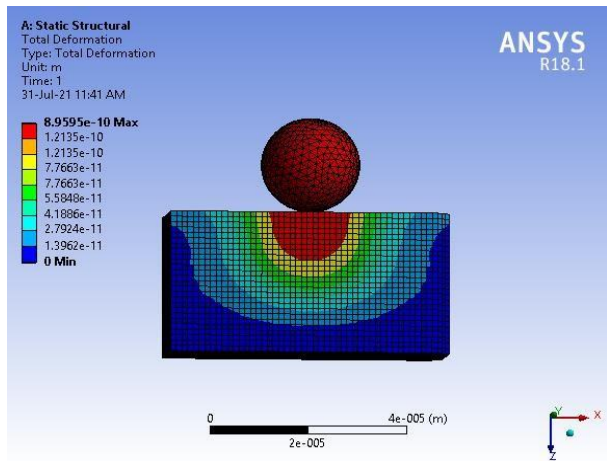
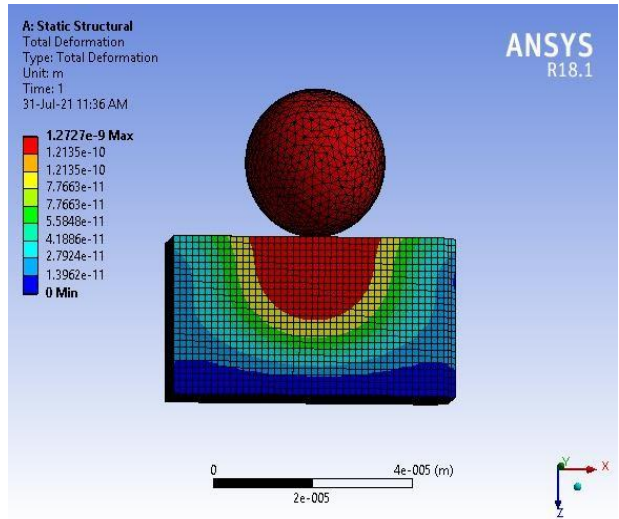
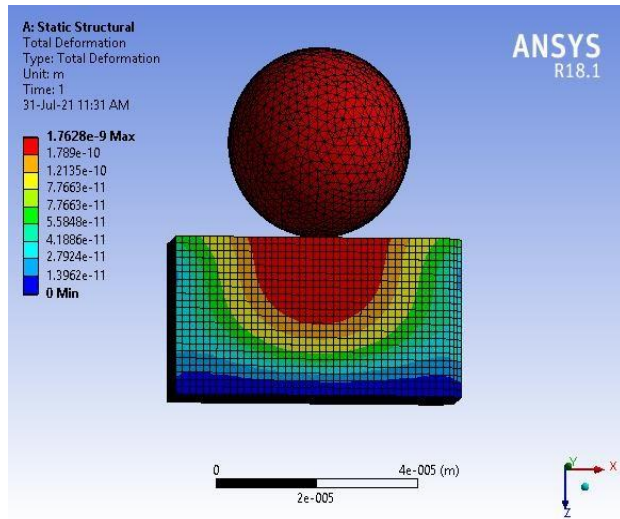


Figure 4-2 Total Deformation at different sizes

#### **4.4 Equivalent Stress at different sizes**

Three dimensional stresses and strains build up in many directions. A common way to express these multi-directional stresses is to summarize them into an “Equivalent” stress, also known as the “Von Mises” stress. Equivalent stress against the impact of 18 $\mu$ m and 5 $\mu$ m alumina is 6.3757e7pa and 1.8447e7 pa respectively. Maximum Safety factor for impact of 10 $\mu$ m alumina at 1 bar pressure is 4.2236e-7. It is clearly noticed that the greater radius in Spherical indentation causes a deeper indentation surface profile.

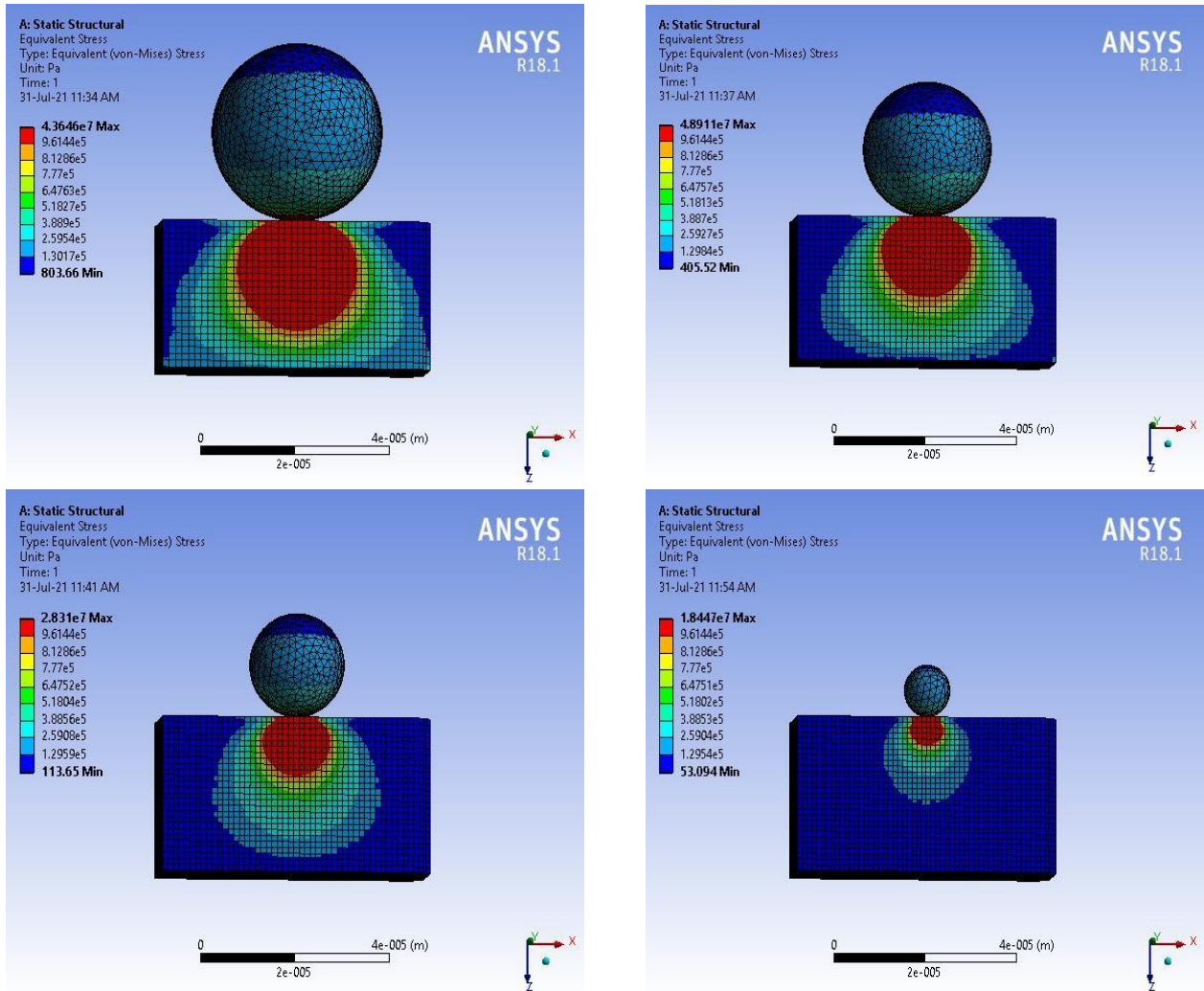


Figure 4-3 Equivalent stress at different sizes

## 4.5 Total Deformation at different forces

Total deformation in fused silica at constant size of alumina but different forces. The maximum total deformation at  $10\mu\text{m}$  alumina with 8 bar and 1 bar pressure is  $1.7919 \times 10^{-9}$  m and  $7.1676 \times 10^{-9}$  m respectively. According to Hertz depth of deformation is directly proportional to load. I observed in my ansys based results the depth of deformation is increased with load. According to Hertz equation this model is valid.

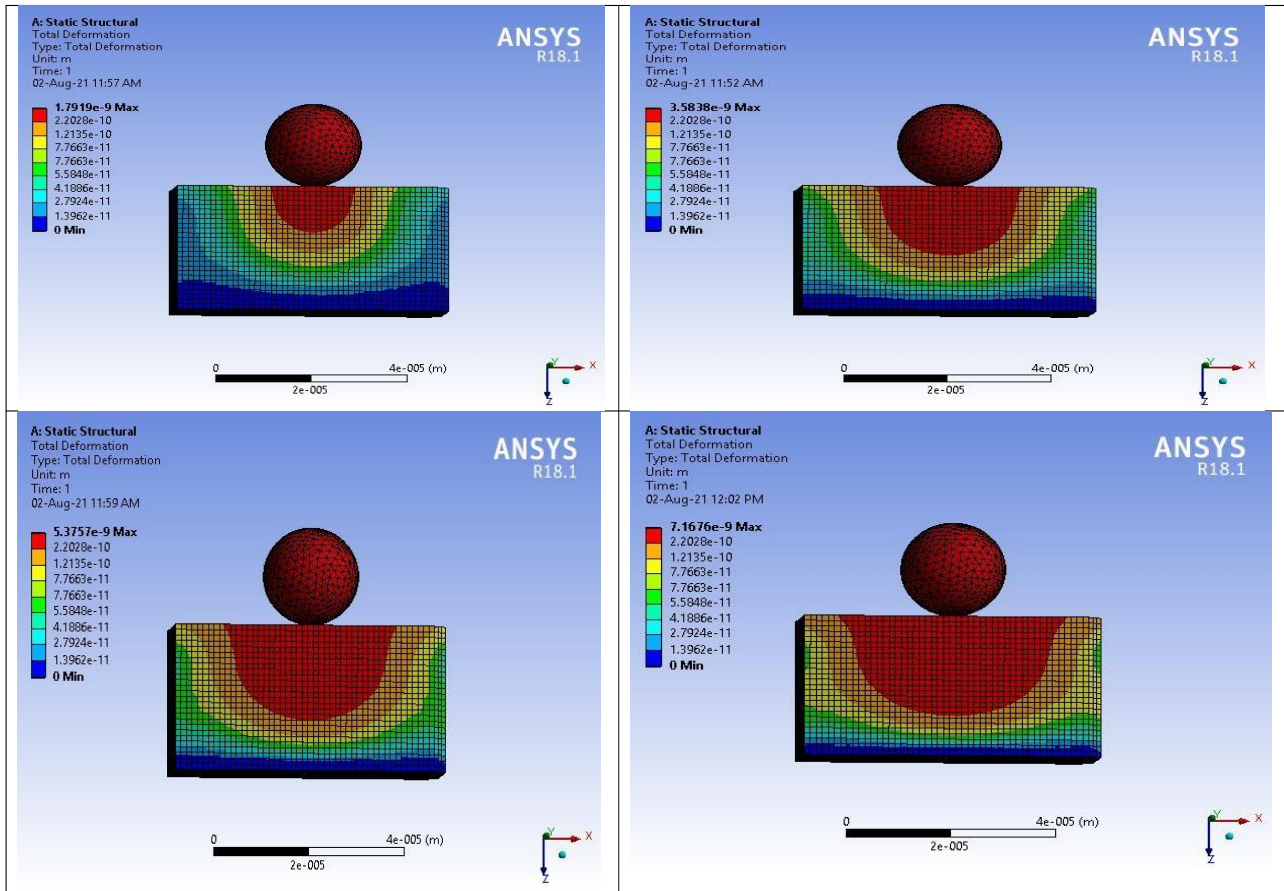


Figure 4-4

Figure 4-4 Total Deformation at different forces

## 4.6 Equivalent Stress at different forces

By the impact of  $10 \mu\text{m}$  alumina with 8 and 2 bar pressure Maximum Equivalent stress is  $5.66 \times 10^{-7}$  pa and  $2.2608 \times 10^{-8}$  pa respectively. Its observed that The indenter load increases with the increasing radius due to the increased contact area with the material. The greater radius in Spherical indentation causes a deeper indentation surface profile.

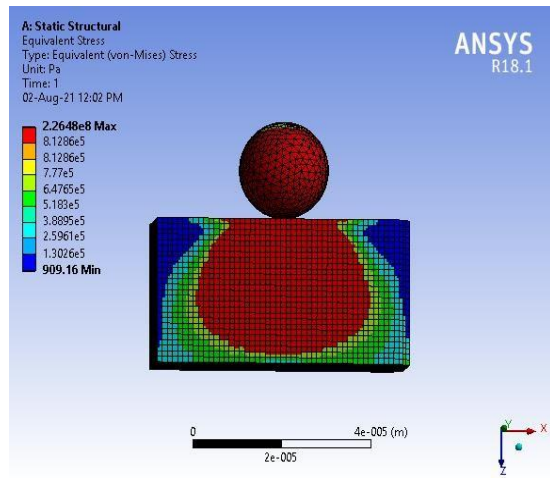
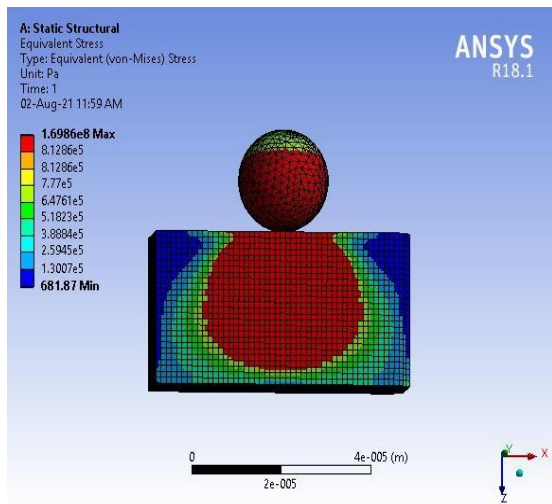
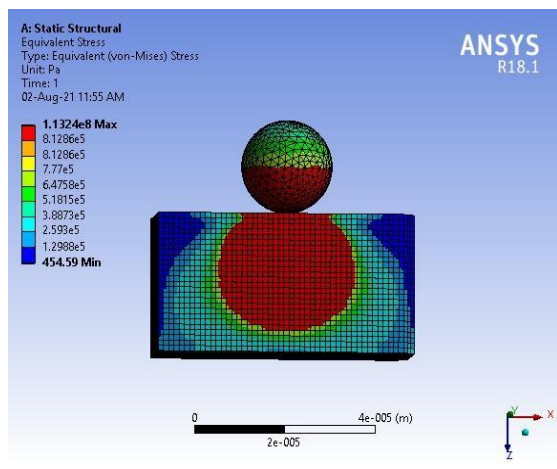
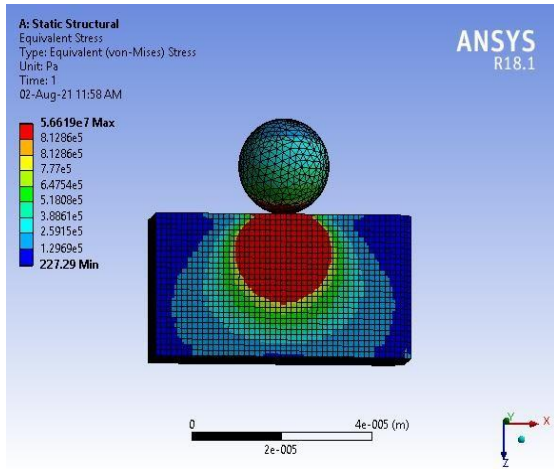


Figure 4-5 Equivalent stress at different forces

## 4.7 Comparison of FEA result with Experiments:

In general a directly modeling an indentation experiment using FEA should produce a more accurate estimate of indentation stress than the simple hertz's approximation. However it should be understood that there are computational difficulties with 3D FEA which prohibit a completely faithful virtual representation of the experiment. The governing equation clearly shows that initiation and growth of cracks is directly proportional to applied load on indenters. Figure 4.7 shows the measured load-displacement curves for all analyzed indentation experiments using spherical indenters. Our work showed that simulation using spherical indenters matched the experimental results.

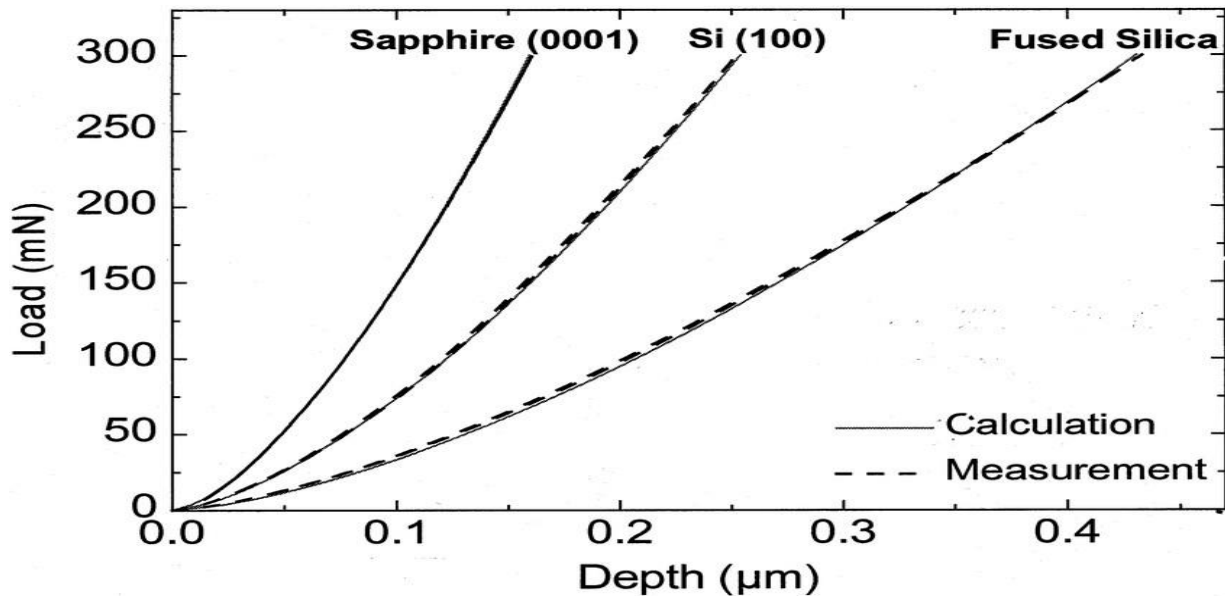


Figure 4-6 Comparison between calculated and measured load-depth data for three materials.

## 4.8 Pressure vs Total Deformation Curve:

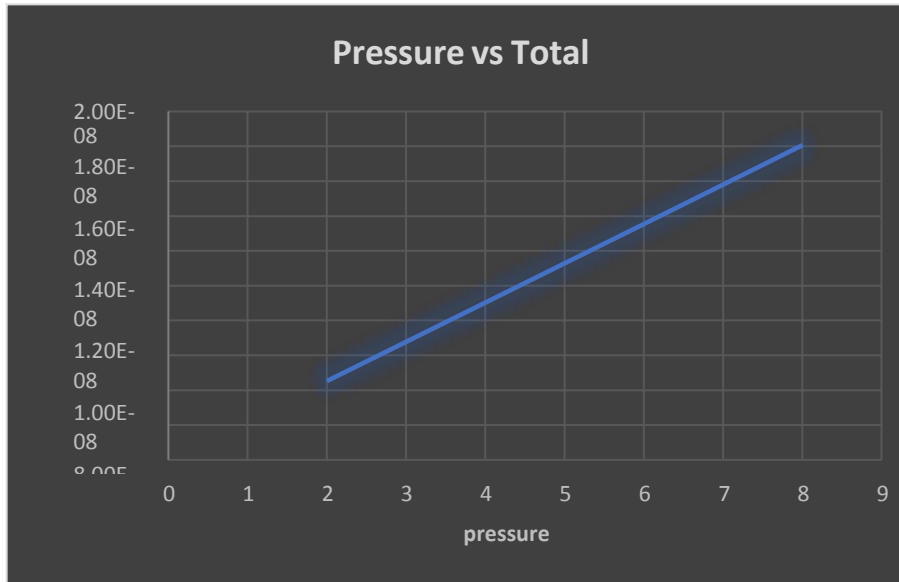


Figure 4-7 Pressure vs Total Deformation Curve model 5-8

# Conclusion

The focus of this study was to better understand how fused quartz cracks on the small-scale due to contact and impact using Spherical indenters with various sizes and loads. From the surface and subsurface cracking analysis, conclusions can be drawn about the formation and evolution of cracks in fused quartz:

It is clearly noticed that the indenter load increases with the increasing radius due to the increased contact area with the material. The greater radius in Spherical indentation causes a deeper indentation surface profile. In addition, the indenter tip with a larger diameter will result in a higher Young's modulus and higher hardness, while a larger plastic zone size can be formed with a sharper indenter due to the higher stress concentration employed. A FEM parametric study was performed using different contact geometries to examine the effect of load on displacement. This work introduced basic procedures of indentation simulation using finite element method. The relationship between load and indentation depth was obtained. The agreement between the numerical results and experimental data was satisfactory to some extent. It was shown that FEM is an effective tool for simulation of optical indentation test. However, limitation caused by simplification of models and assumptions should not be neglected. With the rapid development of nano-scale mechanics and new numerical analysis methods, nowadays 2-D finite element modeling cannot meet the requirement of precisely simulating indentation testing.

# References

- [1] Hertz H. 1896 *Miscellaneous papers*, ch. 5 and 6. Translated by DE Jones and GH Schott. London, UK: Macmillan and Co Ltd.
- [2] Auerbach F. 1891 On the absolute measurement of hardness. *Ann. Phys. Chem.* **43**, 61–100. (doi:10.1002/andp.18912790505)
- [3] Tolansky S, Howes VR. 1954 Optical studies of ring cracks on glass. *Proc. Phys. Soc. Lond.* **B67**, 467–472. (doi:10.1088/0370-1301/67/6/303)
- [4] Benbow JJ. 1960 Cone cracks in fused silica. *Proc. Phys. Soc. Lond.* **75**, 697–699. (doi:10.1088/0370-1328/75/5/308)
- [5] Tillett JPA. 1956 Fracture of glass by spherical indenters. *Proc. Phys. Soc. Lond.* **B69**, 47–54. (doi:10.1088/0370-1301/69/1/306)
- [6] Roesler FC. 1956 Brittle fracture near equilibrium. *Proc. Phys. Soc. Lond.* **B69**, 981–992. (doi:10.1088/0370-1301/69/10/303)
- [7] Chaudhri MM, Yoffe EH. 1981 The area of contact between a small sphere and a flat surface. *Philos. Mag.* **A44**, 667–675. (doi:10.1080/01418618108236169)
- [8] Wilshaw TR. 1971 The Hertzian fracture test. *J. Phys. D.* **4**, 1567–1581. (doi:10.1088/0022-3727/4/10/316)
- [9] Chen SY, Farris TN, Chandrasekar S. 1995 Contact mechanics of Hertzian cone cracking. *Int. J. Solids Struct.* **32**, 329–340. (doi:10.1016/0020-7683(94)00127-I)
- [10] Zhuang, C.Q., Z.P. Li, and S.S. Lin, Counter-intuitive experimental evidence on the initiation of radical crack in ceramic thin films at the atomic scale. *AIP Advances*, **2015**. **5**(10).

- [11] Tandon, R. and R. E. Cook, Cone crack nucleation at sharp contacts. *Journal of the American Ceramic Society*, **1992**. **75**(10): p. 2877-2880.
- [12] Luo, J., et al., Crack nucleation criterion and its application to impact indentation of glasses. *Scientific Reports*, **2016**. **6**.
- [13] Cuadrado, N., et al., Geometry of nanoindentation cube-corner cracks observed by FIB tomography: Implication for fracture resistance estimation. *Journal of the European Ceramic Society*, **2015**. **35**(10): p. 2949-2955.
- [14] Johanns, K. E. et al., Anevaluation of the advantages and limitations in simulating indentation cracking with cohesive zone finite elements. *Modelling and Simulation in Materials Science and Engineering*, **2014**. **22**(1): p. 015011.
- [15] Elfallagh, F. and B. J. Inkson, 3D analysis of crack morphologies in silicate glass using FIB tomography. *Journal of the European Ceramic Society*, **2009**. **29**(1): p. 47-52.
- Harding, D. S., Cracking in brittle materials during low-load indentation and its relation to fracture toughness, in *Materials Science and Engineering*. 1995, Rice University. p. 225.
- [16] Morris, D. J., S. B. Myers, and R. F. Cook, Sharp probes of varying acuity: Instrumented indentation and fracture behavior. *Journal of Materials Research*, **2004**. **19**(1): p. 165-175.
- [17] Jang, J. and G. M. Pharr, Influence of indenter angle on cracking in Si and Ge during nanoindentation. *Acta Materialia*, **2008**. **56**(16): p. 4458-4469.
- [18] Gross, T. M., Deformation and cracking behavior of glasses indented with diamond tips of various sharpness. *Journal of Non-Crystalline Solids*, **2012**. **358**(24): p. 3445-3452.
- [19] Pharr, G. M., Measurement of mechanical properties by ultra-

- low load indentation. *Materials Science and Engineering: A*, **1998**, **253**(1-2):p.151-159.
- [20] Lawn, B.R., A.G. Evans, and D.B. Marshall, Elastic/plastic indentation damage in ceramics: The median/radial crack system. *Journal of the American Ceramic Society*, **1980**, **63**(9-10):p.574- 81.
- [21] Cuadrado, N., et al., Evaluation of fracture toughness of small volumes by means of cube-corner nanoindentation. *Scripta Materialia*, **2012**, **66**(9):p.670-673.
- [22] Laugier, M.T., New formula for indentation toughness in Ceramics. *Journal of Materials Science Letters*, 1987, **6**(3):p.355-356.
- [23] Hyun, H.C., et al., Evaluation of indentation fracture toughness for brittle materials based on the cohesive zone finite element method. *Engineering Fracture Mechanics*, **2015**, **134**:p.304-316.
- [24] Ma, D.J., et al., New method for extracting fracture toughness of ceramic materials by instrumented indentation test with Berkovich indenter. *Journal of the European Ceramic Society*, **2017**, **37**(6):p.2537-2545.
- [25] Mata, M., O. Casals, and J. Alcala, The plastic zone size in indentation experiments: The analogy with the expansion of a spherical cavity. *International Journal of Solids and Structures*, **2006**, **43**(20):p.5994-6013.
- [26] Whittle, B.R. and R.J. Hand, Morphology of Vickers indentation flaws in soda-lime silicate glass. *Journal of the American Ceramic Society*, 2001, **84**(10):p.2361-2365.
- [27] Xie, Z.H., et al., Subsurface indentation damage on ceramics. *Journal of the American Ceramic Society*, **2004**, **87**(11):p.2114-2124.
- [28] Munroe, P.R., The application of focused ion beam microscopy in the material sciences. *Materials*

1 sCharacterization,2009.**60**(1):p.2-13.

[28] B.Lawn“FractureofBrittleSolids,-SecondEdition,Chapter2”Cambridge  
UniversityPress, **1993**